

## Giant Resonances in the Doubly Magic Nucleus $^{48}\text{Ca}$ from the $(e, e'n)$ Reaction

S. Strauch,\* P. von Neumann-Cosel, C. Rangacharyulu,<sup>†</sup> A. Richter, G. Schrieder, K. Schweda, and J. Wambach

*Institut für Kernphysik, Technische Universität Darmstadt, D-64289 Darmstadt, Germany*

(Received 11 April 2000)

The  $^{48}\text{Ca}(e, e'n)$  reaction has been investigated for excitation energies 11–25 MeV and momentum transfers  $0.22\text{--}0.43\text{ fm}^{-1}$  at the superconducting Darmstadt electron linear accelerator S-DALINAC. Electric dipole and quadrupole plus monopole strength distributions are extracted from a multipole decomposition of the spectra. Their fragmented structure is described by microscopic calculations allowing for coupling of the basic particle-hole excitations to more complex configurations. Comparison of the excitation spectrum of the residual nucleus  $^{47}\text{Ca}$  with statistical model calculations reveals a 39(5)% contribution of direct decay to the damping of the giant dipole resonance.

PACS numbers: 24.30.Cz, 21.60.Jz, 25.30.Fj, 27.40.+z

Giant multipole resonances are fundamental manifestations of collective behavior in the atomic nucleus. Despite considerable experimental and theoretical research on these elementary modes, our understanding is still limited [1–3]. While compact strength is found for the lowest multipolarities in heavy nuclei and the systematics of its energy dependence is reasonably well established and theoretically fairly well understood, the complex strength distributions observed in light and medium-mass nuclei still represent a challenge to theory. The most developed microscopic models are based on extensions of the random phase approximation (RPA) which works best at shell closures [1]. Accordingly, data in doubly magic nuclei provide benchmarks for their experimental test.

In view of this importance the almost complete lack of experimental information on giant resonances in the doubly closed-shell nucleus  $^{48}\text{Ca}$  comes as a surprise. Here, new results on the isovector giant dipole resonance (IVGDR) and the isoscalar giant monopole (ISGMR) and quadrupole (ISGQR) modes in  $^{48}\text{Ca}$  are reported using coincident electron scattering. This method combines several favorable aspects for nuclear structure studies. Effects of the well-understood electromagnetic interaction can be separated from the genuine nuclear structure information, unlike for hadronic probes with their complicated reaction mechanisms. Furthermore, the coincidence condition removes the radiative tail from elastic scattering, thereby providing a nearly background-free response.

Since the giant multipole strengths typically lie in the continuum, i.e., above particle thresholds, the dominant relaxation mechanism is another subject of high interest. A competition between direct single-particle emission from the initially excited particle-hole states and mixing into a dense background of complex multiparticle-multihole configurations is expected, but the quantitative role of both processes is not clear. Again, results in  $^{48}\text{Ca}$  would be of particular interest because  $^{48}\text{Ca}$  represents (besides  $^{208}\text{Pb}$ ) the best shell-model nucleus known.

So far, experiments of the type  $(e, e'x)$  have mainly concentrated on charged particle emission which dominates in lighter nuclei [4–11]. The coincident detection of neutrons

in the hostile environment of an electron accelerator represents a considerable experimental task, and only a few exploratory investigations have been performed [12–17]. The present results have been obtained with a new setup for  $(e, e'n)$  reactions developed at the S-DALINAC. In  $^{48}\text{Ca}$ , because of the low threshold ( $E_n = 9.98\text{ MeV}$ ), neutron decay dominates the continuum emission in the giant resonance excitation region.

Data were taken at electron energies (angles)  $E_0 = 67.7, 88.0\text{ MeV}$  ( $\Theta_e = 40.0^\circ$ ) and  $E_0 = 87.7, 103.4\text{ MeV}$  ( $\Theta_e = 52.1^\circ$ ), corresponding to momentum transfers  $q = 0.22, 0.29, 0.36,$  and  $0.43\text{ fm}^{-1}$ , respectively. The metallic Ca target enriched to 92.5%  $^{48}\text{Ca}$  had an areal density of  $17\text{ mg/cm}^2$ . Beam currents were limited to about 100–400 nA in order to ensure reasonable true-to-random coincidence rates around one to one. A large solid angle magnetic spectrometer was used for electron detection [9]. Excitation energies in  $^{48}\text{Ca}$  up to 25 MeV were covered. Decay neutrons were detected with six NE213 liquid scintillator counters placed at angles between  $0^\circ$  and  $90^\circ$  (one at about  $180^\circ$ ) relative to the recoil momentum axis of  $^{47}\text{Ca}$ . The distance of the detectors to the target was 80 cm, subtending a solid angle of about 20 msr. The calibration procedure including rescattering corrections from the complex neutron and gamma shielding is described in [18].

An integration over all emission angles was performed to deduce the fraction of the total  $(e, e')$  cross section coincident with neutron decay. Here, for simplicity we take the average over the six measured emission angles. The angular correlations exhibit little structure with typical variations of no more than 20% in the cross sections. For selected examples the validity of the simple method was tested against results obtained using a Legendre polynomial fit. Further corrections for the threshold energy in the neutron detection of about 1 MeV and the contributions of two-neutron emission above 17.22 MeV were applied by using statistical model calculations with the code CASCADE [19]. An example of the resulting spectra is displayed in Fig. 1. At the corresponding momentum transfer the cross section is dominated by the IVGDR with a

maximum about 19 MeV. Because of the good energy resolution of about 70 keV full width at half maximum, considerable fine-structure is visible up to the highest energies. In particular, a sharp resonance, whose nature is discussed briefly below, can be identified at a very high energy,  $E_x = 24.2$  MeV.

The form factor of the excitation strength in  $^{48}\text{Ca}$ , summed over excitation energies from 11 to 20 MeV, is displayed in Fig. 2(a). The dashed and dotted lines are theoretical  $E1$  and  $E2$  form factors constructed from the RPA transition densities of [20]. A fit of their weighted sum (solid line) to the data determines the coefficients for a decomposition into the relative  $E1$  and  $E2$  cross section parts. By extrapolation to the photon point these can be converted to the transition strengths presented in Figs. 2(b) and 2(c). Note that, due to the similarity of collective  $E0$  and  $E2$  form factors, only the sum of both multipolarities can be determined from the data. We next discuss the determined strength distributions in detail.

An important measure of collective excitation is a model-independent energy-weighted sum rule (EWSR). For the analyzed excitation energy range  $E_x = 11$ –25 MeV we find an exhaustion of 81(12)% for the IVGDR and 72(11)% of the ISGQR. The latter value represents an unknown mixture of monopole and quadrupole parts. At the photon point the cross section corresponds to  $B(E2) + \frac{25}{16\pi}B(E0)$ , which can be derived exactly in plane wave Born approximation but should also approximately hold in distorted wave Born approximation [12]. Thus, assuming, e.g., equal exhaustion of the ISGMR and ISGQR, the number given above would translate to 46(6)% of the respective EWSR's.

Next we discuss the comparison with other experimental information. The IVGDR in  $^{48}\text{Ca}$  has been measured in photoabsorption reactions [21]. The corresponding  $B(E1)$  strength distribution (solid circles) is compared in Fig. 2(b) with the present result. Although showing less detail because of the limited resolution, the global

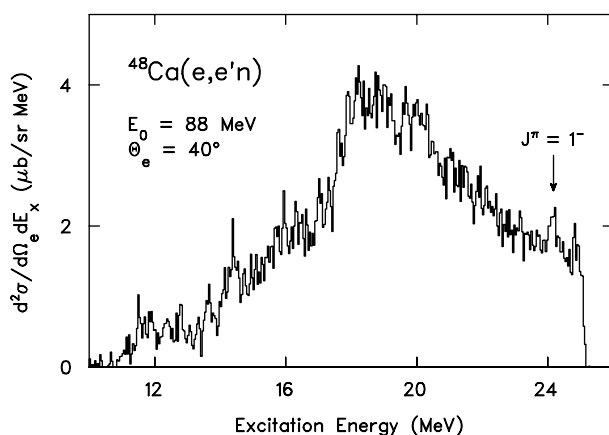


FIG. 1. Excitation spectrum of  $^{48}\text{Ca}$  for the  $(e, e'n)$  reaction at  $E_0 = 88.0$  MeV and  $\Theta_e = 40^\circ$  after integration over all neutron emission angles. The arrow indicates a sharp resonance at  $E_x = 24.2$  MeV.

variation is in agreement with the results of the  $(e, e'n)$  experiment. The difference in absolute magnitude is still within the systematic uncertainties of both experiments. The summed monopole and quadrupole strengths displayed in Fig. 2(c) exhibit an almost flat distribution from the onset at about 12 MeV to the highest energy studied in the present experiment. Evidence for similar highly fragmented  $E0$  and  $E2$  strength distributions has also been found in the doubly magic nucleus  $^{40}\text{Ca}$  [9]. Some information is available on the non-spin-flip,  $\Delta L = 2$  cross sections from a polarized proton scattering experiment on  $^{48}\text{Ca}$  [22] which would correspond to the ISGQR. However, both the energy resolution and the limited accuracy of the  $(\vec{p}, \vec{p}')$  data preclude a detailed comparison with the present  $(e, e'n)$  results.

In contrast to the experimental results, RPA calculations predict a compact ISGMR and ISGQR in Ca nuclei (see, e.g., Ref. [1]). For an understanding of the experimental observations, one thus has to invoke the coupling to more complex degrees of freedom. One quite successful approach based on Green function methods allows for the inclusion of particle-hole ( $p$ - $h$ ) configurations coupled to low-lying collective vibrations and the ground-state (GS)

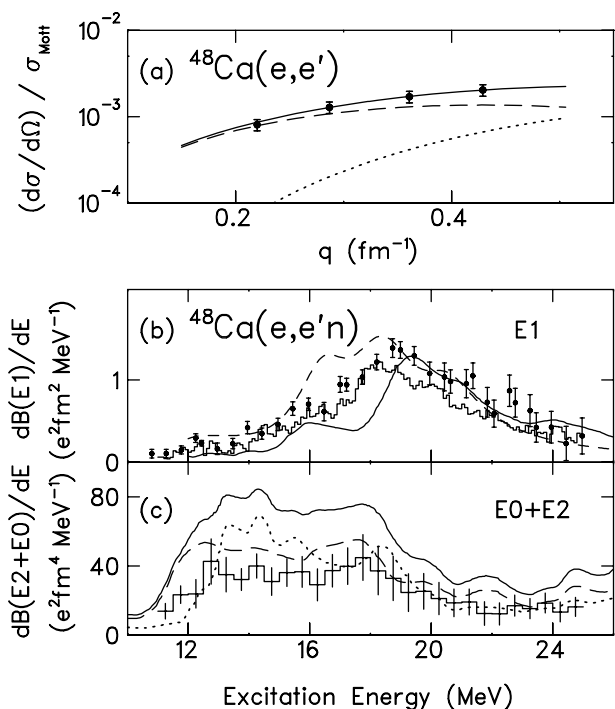


FIG. 2. (a) Form factor of the  $^{48}\text{Ca}(e, e'n)$  reaction summed for  $E_x = 11$ –20 MeV. The dashed and dotted lines are RPA predictions for the IVGDR and the ISGQR, respectively, in  $^{48}\text{Ca}$  using transition densities of [20] and normalized such that the sum (solid line) describes the data. (b)  $B(E1)$  strength distribution. Solid circles are the results of a photoabsorption measurement [21]. The solid and dashed lines are microscopic calculations of [25] and [20]. (c)  $B(E0) + B(E2)$  strength distribution. The short-dashed, long-dashed, and solid lines show the predictions of [25] for  $B(E0)$ ,  $B(E2)$ , and their sum, respectively.

correlations induced by them [23]. Within this model, the experimental findings for  $^{40}\text{Ca}$  of significant  $E0$  and  $E2$  strengths at excitation energies well below the main RPA peak could be traced back to the additional GS correlations [24]. Application of this model to giant resonances in  $^{48}\text{Ca}$  has been reported in [25]. The predicted  $B(E1)$  distribution is included as the solid line in Fig. 2(b). Except for an overall shift of about 1 MeV towards higher energies, good agreement is found for the shape and the absolute magnitude.

One may note that the calculation includes a folding with a Gaussian of width  $\Delta = 0.5$  MeV while the energy resolution of the  $(e, e'n)$  experiment was much better. Results of similar quality for the IVGDR can be obtained from continuum RPA calculations when allowing for large energy averaging parameters. Thus, the gross structure is already determined by the Landau damping. As an example, the GDR strength in  $^{48}\text{Ca}$  provided by [20] is presented as a dashed line in Fig. 2(b) after folding with  $\Delta = 1$  MeV. Again, the global features of the distribution are well accounted for. The prediction of the overall strength exceeds the data by roughly 20%, probably due to the large exchange term in the interaction used in [20]. It would be interesting to see whether the more refined calculations of [25] could eventually provide an explanation of the experimentally observed fine-structure.

Model results of [25] for the  $(E2 + E0)$  strength are shown Fig. 2(c). The strong spreading and the concentration of strength at low energies,  $E_x \approx 13\text{--}18$  MeV are satisfactorily reproduced. The calculations indicate comparable contributions of  $E0$  and  $E2$  strength with local maxima shifted relative to each other, thereby leading to the rather leveled-out distribution. However, the absolute magnitude is overpredicted by a factor of 2. This large discrepancy is difficult to understand in view of the almost perfect description [24] of the corresponding strength distribution in  $^{40}\text{Ca}$  deduced from  $(e, e'x)$  experiments [9]. We remark, however, that the results of [25] predict about twice as much  $E0$  strength in the studied energy interval than previous calculations by the same authors within the same approach [26].

We now turn to another central question of giant resonance studies, viz., understanding the role of direct and statistical contributions to the decay. Here, electroinduced coincidence experiments provide unique possibilities. The experiment is kinematically complete, so one can reconstruct the excitation spectrum of the residual nucleus  $^{47}\text{Ca}$  populated in the  $^{48}\text{Ca}(e, e'n)$  reaction. Since  $E1$  excitations dominate in the investigated momentum transfer range, we choose as an example the lowest measured momentum transfer value, where contributions from other multipoles can be neglected. Excitation of the GS and well-known low-lying levels of  $^{47}\text{Ca}$  can be clearly identified in Fig. 3. The shaded area displays the prediction of statistical model calculations with CASCADE modified [27] to take isospin properly into account. The calculation is normalized so as not to overshoot the data.

At higher  $^{47}\text{Ca}$  energies good agreement is found, but the experimental population of the GS and a group of  $1/2^+$  and  $3/2^+$  levels at about 2.6 MeV strongly exceeds the statistical expectations. Their wave functions exhibit a rather pure single-hole character with respect to the neutron-closed shell in  $^{48}\text{Ca}$  [28].

A check of the statistical model results is provided by the good description of the decay to the first excited  $^{47}\text{Ca}$  level at 2.014 MeV with  $J^\pi = 3/2^-$  which has a more complicated structure with large  $(1p\text{-}2h)$  components [29]. The excess population of single-hole states in  $^{47}\text{Ca}$  is therefore interpreted as the signature of direct decay contributions. It corresponds to 39(5)% of the total  $E1$  strength in  $^{48}\text{Ca}$ . This fraction is found to be independent of excitation energy within the experimental uncertainties. Large decay contributions of the IVGDR resonance were also observed in  $^{40}\text{Ca}$  [9] and generally in  $sd$ -shell nuclei [30]. The present results indicate an extension of this feature into the  $fp$  shell (see also Ref. [31]). In passing we note that information on the damping process is also contained in the fine-structure (see Fig. 1), as demonstrated recently for the example of the ISGQR in  $^{208}\text{Pb}$  [32].

Finally, we briefly comment on the observation of a sharp resonance in  $^{48}\text{Ca}$  at a very high energy of 24.2 MeV (see Fig. 1). The small width implies an isobaric analog resonance (IAR), and the momentum transfer dependence favors an electric dipole character of its excitation. Thus, quantum numbers  $J^\pi; T = 1^-; 5$  are suggested. The  $T_> = T_0 + 1$  isospin character of the level, where  $T_0$  is the isospin of the GS, is further confirmed by its decay properties. Figure 4 depicts the energy spectrum of the residual nucleus for a  $^{48}\text{Ca}$  excitation energy interval around the resonance. The shaded area again represents the predictions for statistical decay. Good agreement is found for higher  $^{47}\text{Ca}$  energies. A peak at  $E_x(^{47}\text{Ca}) = 12.7$  MeV stands out clearly from the otherwise smooth spectrum. It results from the decay of

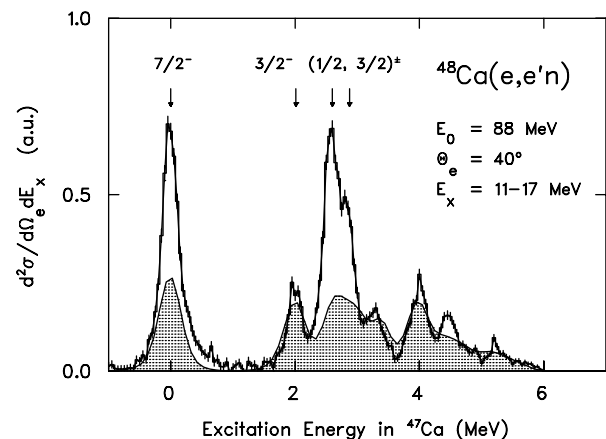


FIG. 3. Population of states in the residual nucleus  $^{47}\text{Ca}$  through the  $^{48}\text{Ca}(e, e'n)$  reaction for kinematics favoring excitation of the IVGDR. The shaded area represents the statistical model expectations.

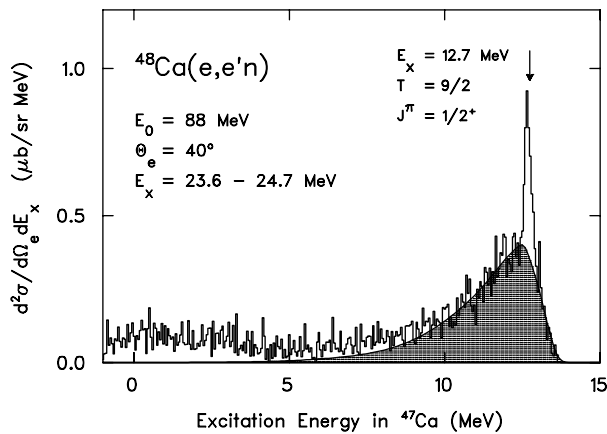


FIG. 4. Decay of the isobaric analog resonance at 24.2 MeV in  $^{48}\text{Ca}$  to the lowest  $T_{>}$  level in  $^{47}\text{Ca}$  at 12.7 MeV. The shaded area represents the statistical model expectations.

the IAR to the lowest  $T_{>}$  level in  $^{47}\text{Ca}$  at 12.7 MeV with  $J^\pi; T = 1/2^+; 9/2$  [33]. The width of about 250 keV is in accordance with the resolution of the neutron detectors for that energy. Corresponding spectra generated from  $^{48}\text{Ca}$  energy intervals slightly below and above the resonance do not show any pronounced structures. Within the experimental uncertainties, the IAR decays entirely to the  $T_{>}$  level, and no branches to  $T_{<} = T_0$  levels are observed. While the power of the  $(e, e'p)$  reaction for the detailed spectroscopy of IAR in heavy nuclei has recently been demonstrated [34], the present results prove that the same also holds for  $(e, e'n)$  experiments.

To summarize, a study of low-multipolarity giant resonances in  $^{48}\text{Ca}$  with the  $(e, e'n)$  reaction has been presented. The ISGQR and ISGMR resonances exhibit very complex strength distributions. Microscopic RPA results are capable of describing the gross structure of the IVGDR. The calculations of [25] demonstrate that the fragmentation of the electromagnetic  $E0$  and  $E2$  response can be reproduced by inclusion of the coupling to  $1p1h \otimes$  phonon states, but overpredict the total strength by a factor of 2. Further insight into this puzzling result may be obtained from second-RPA calculations which have been shown to account successfully for magnetic resonances in medium-mass nuclei [35]. An extension to electric resonances is presently underway. A large fraction of direct decay from the IVGDR of about 40% is deduced by comparison of the residual nucleus excitation spectrum to statistical model calculations. Finally, we briefly discussed a sharp resonance at high excitation energies in  $^{48}\text{Ca}$  interpreted as  $J^\pi = 1^-$  IAR, providing another impressive example of the power of  $(e, e'x)$  experiments to unravel even fine details of the continuum structure in nuclei.

We are indebted to the S-DALINAC accelerator crew for excellent electron beams, to C. Bähr for his help in the experiment, and to D. Frekers for the loan of the  $^{48}\text{Ca}$

target. I. Hamamoto is thanked for providing us with the transition densities of [20]. This work has been supported by the DFG under Contract No. FOR 272/2-1.

\*Present address: Department of Physics and Astronomy, Rutgers University, Piscataway, NJ 08854.

†Visitor from the Department of Physics, University of Saskatchewan, Saskatoon, S7N5E2 Canada.

- [1] *Electric and Magnetic Giant Resonances in Nuclei*, edited by J. Speth (World Scientific, Singapore, 1991).
- [2] P.F. Bortignon, A. Bracco, and R.A. Broglia, *Giant Resonances: Nuclear Structure at Finite Temperatures* (Harwood Academic, Amsterdam, 1998).
- [3] Special issue on *Topical Conference on Giant Resonances*, Nucl. Phys. **A649** (1999).
- [4] J.R. Calarco *et al.*, Phys. Lett. **146B**, 179 (1984).
- [5] T. Kihm *et al.*, Phys. Rev. Lett. **56**, 2789 (1986).
- [6] A. Tanaka *et al.*, Nucl. Phys. **A489**, 381 (1988).
- [7] J.P. Fritsch *et al.*, Phys. Rev. Lett. **68**, 1667 (1992).
- [8] D. DeAngelis *et al.*, Phys. Rev. Lett. **70**, 2872 (1993); Phys. Rev. C **52**, 61 (1995).
- [9] H. Diesener *et al.*, Phys. Rev. Lett. **72**, 1994 (1994).
- [10] H. Diesener *et al.*, Phys. Lett. B **352**, 201 (1995).
- [11] M. Kohl *et al.*, Phys. Rev. C **57**, 3167 (1998).
- [12] G.O. Bolme *et al.*, Phys. Rev. Lett. **61**, 1081 (1988).
- [13] R.A. Miskimen *et al.*, Phys. Lett. B **236**, 251 (1990); Phys. Rev. C **43**, 1677 (1991).
- [14] C. Takakuwa *et al.*, Phys. Rev. C **50**, 845 (1994).
- [15] T. Saito *et al.*, Phys. Rev. Lett. **78**, 1018 (1997).
- [16] S. Suzuki *et al.*, Phys. Rev. C **60**, 034309 (1999).
- [17] M. Oikawa *et al.*, Phys. Rev. Lett. **84**, 2338 (2000).
- [18] C. Bähr *et al.*, Nucl. Instrum. Methods Phys. Res., Sect. A **411**, 430 (1998).
- [19] F. Pühlhofer, Nucl. Phys. **A280**, 267 (1977).
- [20] I. Hamamoto, H. Sagawa, and X.Z. Zhang, Phys. Rev. C **56**, 3121 (1997).
- [21] G.J. O'Keefe *et al.*, Nucl. Phys. **A469**, 239 (1987).
- [22] F.T. Baker *et al.*, Phys. Rev. C **44**, 93 (1991).
- [23] S. Kamedzhiev *et al.*, Phys. Rev. C **55**, 2101 (1997).
- [24] S. Kamedzhiev, J. Speth, and G. Tertychny, Phys. Rev. Lett. **74**, 3943 (1995).
- [25] S. Kamedzhiev, J. Speth, and G. Tertychny, Nucl. Phys. **A624**, 328 (1997).
- [26] S. Kamedzhiev *et al.*, Nucl. Phys. **A577**, 641 (1994).
- [27] M.N. Harakeh (private communication).
- [28] R. Martin *et al.*, Nucl. Phys. **A185**, 465 (1972).
- [29] T.A. Belote, H.Y. Chen, and O. Hansen, Phys. Rev. **142**, 624 (1966).
- [30] R.A. Eramzhyan *et al.*, Phys. Rep. **136**, 229 (1986).
- [31] B.S. Dolbilkin *et al.*, Z. Phys. A **331**, 107 (1988).
- [32] D. Lacroix *et al.*, Phys. Lett. B **479**, 15 (2000).
- [33] D. Mueller, E. Kachy, and H. Nann, Phys. Lett. **59B**, 233 (1975).
- [34] P. von Neumann-Cosel *et al.*, Phys. Rev. Lett. **78**, 2924 (1997).
- [35] P. von Neumann-Cosel *et al.*, Phys. Rev. Lett. **82**, 1105 (1999).